Content-based Image Retrieval For Surface Defects Of Hot Rolled Steel Strip Using Wavelet-Based LBP

Fatma Zohra BOUDANI [1, 2,*], Nafaa NACEREDDINE[1], and Nacera LAICHE[2]

[1]Research Center in Industrial Technologies CRTI. P.O. Box 64 Cheraga 16014 Algiers, Algeria.
[2] USTHB, Faculty of Electronic and Computing, BP 32 El-Alia, Bab Ezzouar, 16111 Algiers, Algeria.
boudani_f.z@hotmail.com; n.nacereddine@crti.dz; nlaiche@usthb.dz

Abstract. Quality control by artificial vision with applications in industrial manufacturing is a challenging task due to the significant variability of surface defects. In this work, we propose to use content based image retrieval CBIR to manage the large data produced by surface inspection systems. The performance of the CBIR system was evaluated using textural features extracted from NEU database that collects six kinds of surface defects of the hot-rolled steel strip. Different similarity measurements were used to retrieve the most similar images to the query image. The effectiveness of Wavelet based local binary patterns WLBP features was shown in the experimental results for the retrieval of surface defects. WLBP features using Chi square distance achieved the highest retrieval values compared to LBP, GLCM, and EHD features.

Keywords: surface defects, CBIR, hot-rolled steel strip, textural features, feature extraction, wavelet, LBP, Chi square.

1 Introduction

In recent years, products of many industries such as aerospace, marine, automobile, iron and steel industry, electronics, and so on have made huge contributions to the development of the global economy. The competitiveness of manufacturing industry has been accompanied by a large number of surface defects in the final products which is very costly and would lead to enormous economic and reputation losses. Hence, there have been an increasing surface quality control demands for the industrial manufacturing [1-5]. Automatic surface inspection systems produce thousands of defect images on a daily basis. These huge image data are composed of various surface defects with large inter class similarities and intra-class diversities [4]. Therefore, it is very exhausting and time-consuming to analyze all these images on a daily basis. Content based image retrieval (CBIR) systems are suitable tools to handle this problem, since their performance is accurate for large databases with the advantage of bringing human expertise in the decisions making step [6] [7]. The process of CBIR is based on analyzing the visual features of images database such as colors, shapes and texture [6] [8]. In this context, quality control experts use images of serious defects as queries and train the

CBIR system employing features extraction techniques and similarity measurements to retrieve images that look similar to the queries [9] [7]. This will give the experts an overview of the defects occurred in the production lines which will allow them to refine the performance in the future. The industrial surface inspection is mainly a texture analysis problem [2] [4]. Scholars have conducted significant research to inspect local textural irregularities on different types of surfaces such as Steel, stone, textile, wood, and ceramic tiles [1-5]. Publications of the last 3 decades classified texture feature description approaches into four categories, including statistical approaches, filtering based methods, model-based methods, and methods based on machine learning [1-5]. The local binary patterns LBP are a widely used statistical method for describing local texture features of an image by comparing the gray values of every pixel with its neighbors [10]. Many LBP variants have been developed to extract features of various surface defects from images of steel strips [11-14]. In this paper, we present a wavelet based LBP Method WLBP to extract features from hot-rolled steel strip database for an effective retrieval and detection of surface defects.

2 Content based image retrieval

Content based image retrieval CBIR has become an active research field in computer vision. Research interest in this field has increased due to the deployment of large image databases in various professional fields. Accessing requested images from these large and varied image databases is fundamental for the users. Content-based means that the search will analyze the visual features of the image such as colors, shapes, and texture [6]. CBIR systems are created to retrieve images that are visually similar to a query image using two steps [6] [8]:

- Feature Extraction: The first step in the process is extracting features from the image database, allowing the database indexing.
- Matching and comparison: The second step involves matching and comparing these features to yield a result that is similar to the query.

Texture is the most important describing features of industrial surface inspection images [1-5]. It is essentially characterized by the spatial distribution of gray levels in a neighborhood. Textured image contains important information about the structural arrangement of the surface, and the relationship of the surface to the surrounding environment [8].

3 Local binary pattern

The local binary pattern LBP is a widely used method for describing local texture features of an image by comparing the gray values of every pixel with its neighbors. LBP was first introduced by Ojala et al [10]. The original LBP descriptor is defined in a 3×3 window. It uses the gray value of the center pixel (g_c) as a threshold for its 8 neighbors ($g_0, \ldots, g_7$). If the gray value of a neighbor pixel is higher or equal to the threshold than 1 is assigned to this pixel, otherwise it gets 0. The eight binary values will be concatenated in a clockwise direction to form a binary number. Then, the LBP code of the center pixel $g_c(x_c, y_c)$ is obtained by converting the binary number into a decimal number using Equation 1. An example of LBP operator is shown on Fig. 1. The local texture features of the whole image can be described by computing the 256 bins histogram of the LBP codes.

$$\mathrm{LBP}(x_c, y_c) = \sum_{n=0}^{7} 2^n \,\mathrm{sgn}(g_n - g_c) \quad (1)$$

where, $\mathrm{sgn}(g_n - g_c)$ is the sign function defined as

$$\mathrm{sgn}(g_n - g_c) = \begin{cases} 1 \ , g_n \geq g_c \\ 0 \ , g_n < g_c \end{cases} \quad (2)$$

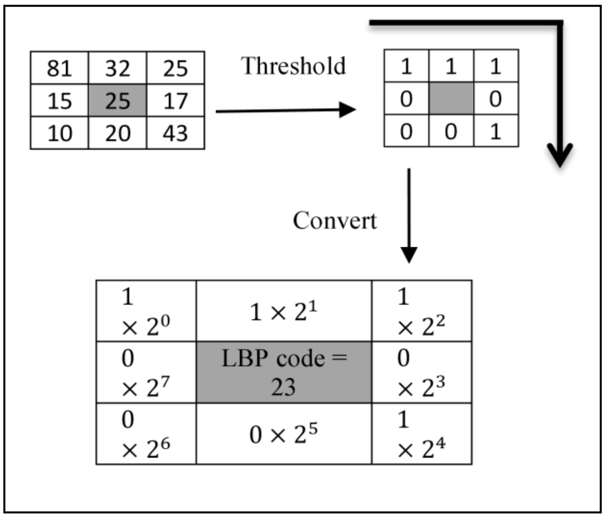

Fig. 1. Example of LBP operator.

4 Image Retrieval Using Wavelet Based Local Binary Patterns

Wavelet transforms have been commonly used in different applications, such as image denoising [15], clustering [16], and features extraction [17-19]. The result of the wavelet transform is a multilevel decomposition of the image into approximation and details coefficients [20]. In this paper, we extract textural features using local binary patterns of the wavelet sub bands. This feature extraction method is the first step of the CBIR process, it consists of the following tasks:

1) Multilevel decomposition of the images via Haar based Discrete Wavelet Transform DWT [20].
2) Computation of LBP codes of the wavelet coefficients (approximation and details).

3) Concatenation of LBP feature vectors of all DWT coefficients to form a single feature vector for each image.

The second step of the process is to compute the similarity between the feature vector of the query image and feature database of the selected descriptor. The similarity measures are then stored and sorted in increasing order and the most similar images are displayed as a retrieval result. The diagram of the proposed image retrieval process is presented in the following figure:

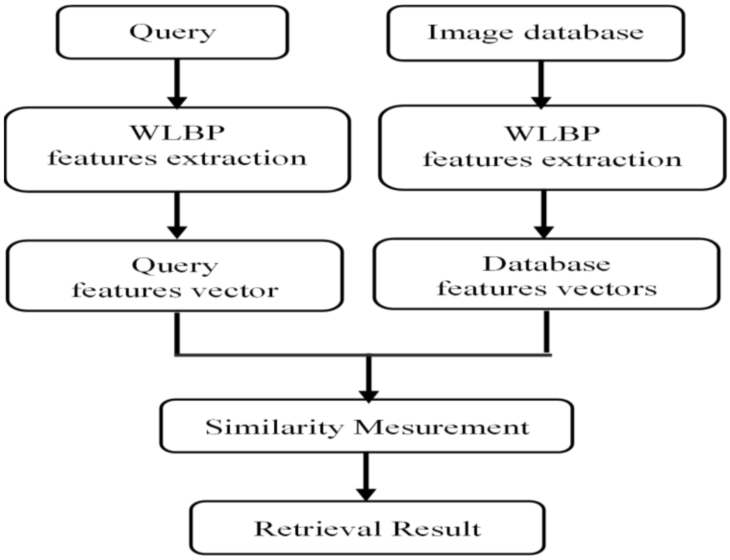

Fig. 2. Diagram of the proposed image retrieval system.

5 Experimental Results

In this section, the performance of WLBP features for content based image retrieval is compared with other feature extraction methods, namely Gray level Co-occurrence matrix (GLCM) [21], Edge Histogram Descriptor (EHD) [22], and the original LBP [10]. We select NEU Surface Defect Database that includes 1,800 gray scale images for experiments [11]. It is an open source dataset comprising six kinds of typical surface defects of the hot-rolled steel strip with 300 images for each defect, i.e., Crazing (Cr), Inclusion (IN), Patches (PA), Pitted Surface (PS), Rolled-in Scale (RS), and Scratches (Sc). Fig. 3 presents samples of the hot-rolled steel surface defects on NEU database. Features databases are constructed by extracting images features from NEU Surface Defect Database using LBP, GLCM features, EHD, and LBP of DWT coefficients.

5.1 Similarity Measurement

We have used Euclidean distance, histogram intersection, Bhattacharyya, and Chi square distance, that are commonly used to measure the similarity between histograms [23] [24]. These distances are obtained as follows.

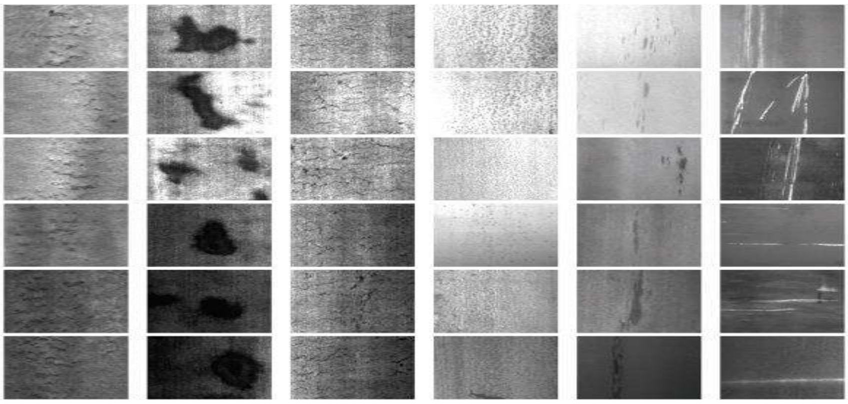

Fig. 3. Steel defects on NEU surface defect database including, from left to right, Rolled-In Scale, Patches, Crazing, Pitted Surface, Inclusion, and Scratches [11].

The Euclidean distance is defined as [25]:

$$D_{Euclidean}(q, x) = \sqrt{\sum_{i=1}^{N}(q - x_i)^2} \tag{3}$$

where, q is the query image feature vector and x is a vector from features database. N represents the total number of element in each feature vector.

The histogram intersection distance is defined as [24]:

$$D(hist_q, hist_x) = \sum_{i=1}^{N} \min(hist_q(i), hist_x(i)) \tag{4}$$

where, $hist_q$ is the histogram-based feature vector of the query image, and $hist_x$ is a vector from the histogram-based features database.

The Bhattacharrya distance between two histograms is defined as [25]:

$$D_{Bhattacharyya}(hist_q, hist_x) = \sqrt{1 - \sum_{i=1}^{N} \frac{\sqrt{hist_q(i).hist_x(i)}}{\sqrt{\sum hist_q(i).\sum hist_q(i)}}} \tag{5}$$

The Chi square distance between two histograms is defined as [24]:

$$D_{chi\ square}(hist_q, hist_x) = \frac{1}{2}\sum_{i=1}^{N} \frac{(hist_q(i) - hist_x(i))^2}{(hist_q(i) + hist_x(i))} \tag{6}$$

The distances are then stored and sorted in increasing order based on similarity distance and most similar images are displayed as a retrieval result.

5.2 Performance evaluation metrics

We have evaluated the retrieval system using the Mean Average Precision (MAP) which is one of the most used metrics in literature to measure the retrieval performances [26]. It is computed as the mean of average precision values for each query. The mathematical representations of the Precision, the Average Precision, and the Mean Average Precision are given below:

- Precision (P) is equivalent to the ratio of retrieved relevant images to the total number of retrieved images N:

$$P(k) = \frac{1}{N}\sum_{k=1}^{N} \mathrm{relevant}(k) \tag{7}$$

  where, relevant (k) is a function that returns 1 if the image at position k is relevant, and returns 0 otherwise.

- The Average Precision (AP) is calculated for a single query by averaging the precision values at each relevant image:

$$AP = \frac{\sum_{k=1}^{N} P(k).\,\mathrm{relevant}(k)}{\text{number of relevant images}} \tag{8}$$

- The MAP for a set of queries Q is given by:

$$MAP = \frac{\sum_{q=1}^{Q} AP(q)}{Q} \tag{9}$$

5.3 Retrieval Results

Experimental results of the proposed system are presented in Table 1. For each descriptor, all images were chosen one by one as a query image and top 10 images were retrieved based on Euclidean distance, Histogram intersection, Chi square, and Bhattacharyya distance. For the WLBP, we have tested up to three levels of the DWT decomposition using Haar wavelet.

According to Table 1, best results in terms of similarity measures were obtained using Chi square, and Bhattacharyya distance. It has been shown that LBP features achieve a good MAP value of 90.26 %; it outperforms both EHD and GLCM features with a MAP difference of about 20 %. Further experiments on WLBP demonstrate the superiority of this descriptor over the previously tested descriptors. Two decomposition levels of the WLBP using Chi square distance yields the highest value of MAP with an improvement of 3 % compared to the results of LBP features. However, a decrease in performance has been detected when using more than two decomposition levels.

Table 1. Comparison of MAP@10 of the selected descriptors using different similarity measures

DISTANCE METRICS	GLCM	EHD	LBP	WLBP 1 level	WLBP 2 levels	WLBP 3 levels
Euclidean distance	0.3721	0.6467	0.8933	0.9104	0.9103	0.9116
Histogram intersection	0.4438	0.6869	0.8211	0.8314	0.8083	0.8283
Bhattacharyya	**0.6834**	0.7032	**0.9026**	**0.9236**	0.9298	0.8871
Chi square	0.5200	**0.7081**	0.8959	0.9216	**0.9329**	**0.9170**

More experiments have been done to assess the performance of the descriptors on each defects class. Table 2 illustrates the MAP values of the top 10 images retrieved based on the Chi Square distance. The CBIR systems using LBP, 1 level WLBP, and 2 levels WLBP features succeed to retrieve all images from the defects class "Rolled in scale" with a MAP value equals to 100%. Two levels WLBP yields the highest MAP values for the classes of Crazing and Patches. The best results for the class of Pitted surface have been achieved by LBP features. However, EHD outperforms the other descriptors in retrieving images of "inclusion", it achieves a MAP value equals to 94.66 % which is higher by more than 7% compared to the closest results obtained by 2 levels WLBP. In addition, even though the total MAP using GLCM features is the worst with a value of 52 %, these features achieve the best MAP score for the class of Scratches. The MAP value of GLCM features is 7 % higher compared to the closest result obtained by 3 levels WLBP.

Table 2. Comparison of retrieval results based on map@10 for different defect classes using chi square.

	MAP@10 Using Chi Square distance					
Defect Classes	**GLCM**	**EHD**	**LBP**	**WLBP 1 level**	**WLBP 2 levels**	**WLBP 3 levels**
Crazing	0.4664	0.8498	0.9680	0.9940	**0.9996**	0.9979
Inclusion	0.3697	**0.9466**	0.8521	0.8677	0.8690	0.8583
Patches	0.4707	0.4985	0.8494	0.9346	**0.9829**	0.9485
Pitted surface	0.3272	0.4219	**0.9453**	0.9413	0.9239	0.8712
Rolled in scale	0.5891	0.8709	**1.0000**	**1.0000**	**1.0000**	0.9988
Scratches	**0.8969**	0.6607	0.7607	0.7917	0.8222	0.8274
Whole database	0.5200	**0.7081**	0.8959	0.9216	**0.9329**	**0.9170**

Retrieval results of a query from the class of patches defects using LBP and 2 levels WLBP are shown in Figure.4 and Figure.5 respectively. Similarity measures using Chi square distance are displayed below each image. The CBIR system using LBP features is not effective for the selected query according to Fig. 4, since it retrieved only 4 relevant images including the query. This retrieval result presents confusion with the class of Crazing defects. The wavelet based LBP performs better with 10 relevant images out of 10 retrieved as shown in Fig. 5.

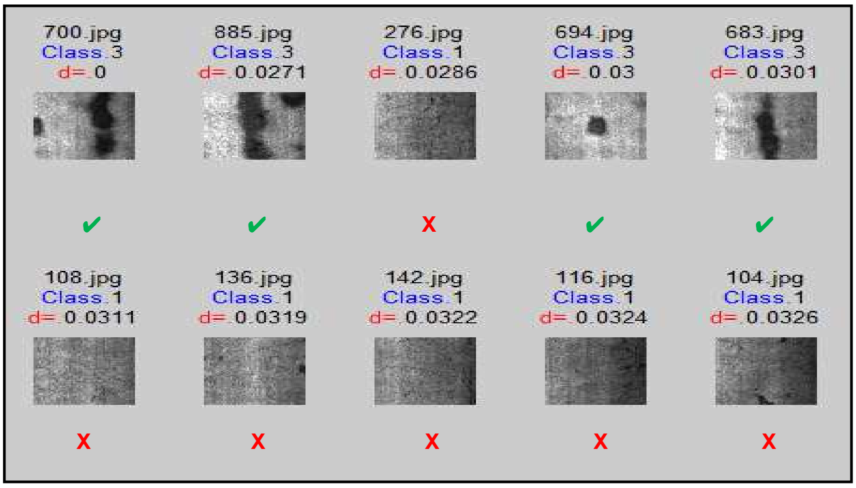

Fig. 4. Image retrieval results for a query (top-left image) of the defect class (Patches) using LBP features.

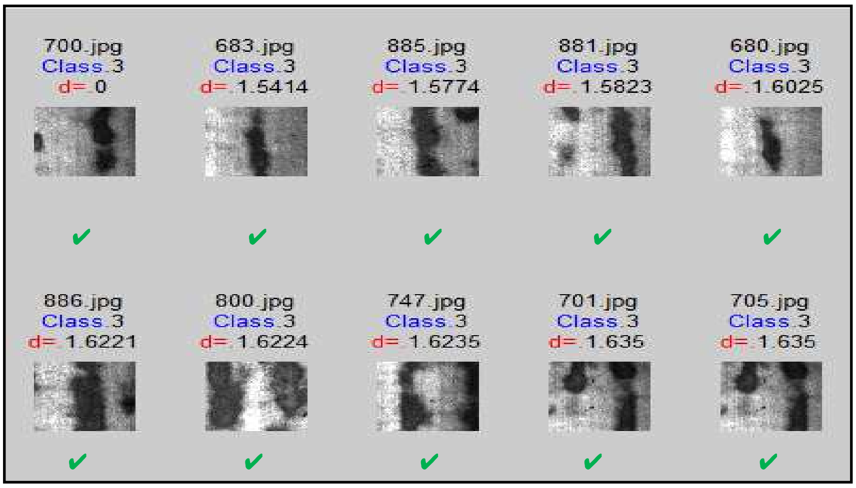

Fig. 5. Image retrieval results for a query (top-left image) of the defect class (Patches) using WLBP features.

To further evaluate the retrieval performance, top 10, 20, 30, 40 and 50 images of the CBIR system using 2 levels WLBP features are retrieved. MAP value is calculated for all the retrieved images of the NEU database based on Chi square, and Bhattacharyya distance. As summarized in Table 3, the best results were obtained using the Chi square distance. In addition, 2 levels WLBP features retain their effectiveness for the entire scope with a MAP value that's greater than 83%.

Table 3. Performance of the wlbp features at five top ranks (10, 20, 30, 40, 50)

WLBP 2 levels	**MAP @10**	**MAP @20**	**MAP @30**	**MAP @40**	**MAP @50**
Chi square	0.9329	0.8930	0.8673	0.8475	0.8306
Bhattacharyya	0.9298	0.8880	0.8603	0.8394	0.8223

6 Conclusion

In this paper, content based retrieval for industrial images of surface inspection was addressed. We compare the retrieval performance of CBIR system using features of LBP, GLCM, EHD, and WLBP. The promising results on the database of hot-rolled steel strip surface defects demonstrate the effectiveness of WLBP features using Chi square distance for industrial images retrieval. Two levels of WLBP outperform the other textural based features and achieve significantly higher mean average precision, especially for the defects classes of Crazing, Patches, and Rolled in scale. In future work, we plan to further boost the retrieval performance by combining descriptors and using features selection techniques. Also, more industrial databases will be considered for evaluation.

References

1. Kumar, A. Computer-vision-based fabric defect detection: A survey. IEEE transactions on industrial electronics, 55(1), 348–363 (2008).
2. Xie, X. A review of recent advances in surface defect detection using texture analysis techniques. ELCVIA: electronic letters on computer vision and image analysis, 1-22 (2008).
3. Karimi, M. H., & Asemani, D. Surface defect detection in tiling Industries using digital image processing methods: Analysis and evaluation. ISA transactions, 53(3), 834–844 (2014).
4. Neogi, N., Mohanta, D. K., & Dutta, P. K. Review of vision-based steel surface inspection systems. EURASIP Journal on Image and Video Processing, (1),1–19 (2014).
5. Luo, Q., Fang, X., Liu, L., Yang, C., & Sun, Y. Automated Visual Defect Detection for Flat Steel Surface: A Survey. IEEE Transactions on Instrumentation and Measurement, 69(3), 626-644 (2020).
6. Eakins, J., & Graham, M. Content-based image retrieval. In Library and Information Briefings. (1999).
7. Iivarinen, J., Rautkorpi, R., Pakkanen, J., & Rauhamaa, J. Content-based retrieval of surface defect images with PicSOM. International Journal of Fuzzy Systems, 6(3), 160 (2004).

8. Juneja, K., Verma, A., Goel, S., & Goel, S. A survey on recent image indexing and retrieval techniques for low-level feature extraction in CBIR systems. In 2015 IEEE International Conference on Computational Intelligence & Communication Technology, pp. 67-72.
9. Nacereddine, N., Ziou, D., & Hamami, L. Fusion-based shape descriptor for weld defect radiographic image retrieval. The International Journal of Advanced Manufacturing Technology, 68(9-12), 2815-2832 (2013).
10. Ojala, T., Pietikäinen, M., & Harwood, D. A comparative study of texture measures with classification based on featured distributions. Pattern recognition, 29(1), 51-59 (1996).
11. Song, K., & Yan, Y. A noise robust method based on completed local binary patterns for hot-rolled steel strip surface defects. Applied Surface Science, 285, 858-864 (2013).
12. Luo, Q., Sun, Y., Li, P., Simpson, O., Tian, L., & He, Y. Generalized completed local binary patterns for time-efficient steel surface defect classification. IEEE Transactions on Instrumentation and Measurement, 68(3), 667-679 (2018).
13. Luo, Q., Fang, X., Sun, Y., Liu, L., Ai, J., Yang, C., & Simpson, O. Surface defect classification for hot-rolled steel strips by selectively dominant local binary patterns. IEEE Access, 7, 23488-23499 (2019).
14. Liu, Y., Xu, K., & Xu, J. An Improved MB-LBP Defect Recognition Approach for the Surface of Steel Plates. Applied Sciences, 9(20), 4222 (2019).
15. Boudani, F. Z., & Nacereddine, N. Diffusion in the wavelet domain for denoising radiographic images of welding defects. In 2019 International Conference on Advanced Electrical Engineering (ICAEE), pp. 1-5. IEEE. Algeria (2019).
16. Chetih, N., Messali, Z., Serir, A., & Ramou, N. Robust fuzzy c-means clustering algorithm using non-parametric Bayesian estimation in wavelet transform domain for noisy MR brain image segmentation. IET Image Processing, 12(5), 652-660 (2018).
17. Moh'd Shamaileh, A., Rassem, T. H., Chuin, L. S., & Al Sayaydeh, O. N. A new feature-based wavelet completed local ternary pattern (Feat-WCLTP) for texture image classification. IEEE Access, 8, 28276-28288 (2020).
18. Chaudhari, C. V. Steel Surface Defect Detection Using Glcm, Gabor Wavelet, Hog, And Random Forest Classifier. Turkish Journal of Computer and Mathematics Education (TURCOMAT), 12(12), 263-273 (2021).
19. Deepa, B., Sumithra, M. G., Kumar, R. M., & Suriya, M. Weiner Filter based Hough Transform and Wavelet feature extraction with Neural Network for Classifying Brain Tumor. In 6th International Conference on Inventive Computation Technologies (ICICT), pp. 637-641. IEEE. India(2021)
20. Shensa, M. J. The discrete wavelet transform: wedding the a trous and Mallat algorithms. IEEE Transactions on signal processing, 40(10), 2464-2482 (1992).
21. Mohanaiah, P., Sathyanarayana, P., & GuruKumar, L. Image texture feature extraction using GLCM approach. International journal of scientific and research publications, 3(5), 1-5 (2013).
22. Won, C. S., Park, D. K., & Park, S. J. Efficient use of MPEG-7 edge histogram descriptor. ETRI journal, 24(1), 23-30 (2002).
23. Cha, S. H., & Srihari, S. N. On measuring the distance between histograms. Pattern Recognition, 35(6), 1355-1370 (2002).
24. Marín-Reyes, P. A., Lorenzo-Navarro, J., & Castrillón-Santana, M. Comparative study of histogram distance measures for re-identification. arXiv preprint arXiv:1611.08134. (2016).
25. Rahman, M. M., Bhattacharya, P., & Desai, B. C. Similarity searching in image retrieval with statistical distance measures and supervised learning. In International Conference on Pattern Recognition and Image Analysis 2005, pp. 315-324. Springer, Berlin, Heidelberg.
26. Deselaers, T., Keysers, D., & Ney, H. Features for image retrieval: an experimental comparison. Information retrieval, 11(2), 77-107 (2008).